IET Control Theory & Applications

Brief Paper

A triple-step non-linear control for path following of autonomous vehicles with uncertain kinematics and dynamics

ISSN 1751-8644
Received on 30th May 2017
Revised 31st August 2017
Accepted on 14th September 2017
E-First on 10th October 2017
doi: 10.1049/iet-cta.2017.0539
www.ietdl.org

Yulei Wang[1], Ning Bian[2], Jingyu Li[3], Jingxin Yuan[1], Hong Chen[1] ✉
[1]*State Key Laboratory of Automotive Simulation and Control, Jilin University, Changchun 130025, People's Republic of China*
[2]*Dongfeng Technical Center, Dongfeng Motor Corporation, Wuhan 430056, People's Republic of China*
[3]*Changchun Institute of Optics, Fine Mechanics and Physics, Chinese Academy of Sciences, Changchun 130033, People's Republic of China*
✉ *E-mail: chenh@jlu.edu.cn*

Abstract: The authors investigate the control problem for autonomous vehicle with both the uncertain kinematics and dynamics. The authors propose a triple-step control scheme to realise the objective of the path following irrespective of the uncertain kinematics and dynamics. The proposed control strategy has the desirable modularisation property that yields an explicit expression without the expense of complicated control structure. The performance of the proposed controller is shown by benchmark simulations.

1 Introduction

Mobility is a fundamental desire of mankind. Automobile production greatly contributes to the quality of life and economic success, but takes the price of resource consumption, noise and exhaust pollution, traffic congestion and fatal traffic incidents as a personal safety risk. Today, the focus of the mobility industry is partly shifting towards emerging markets of advanced driver assistance systems [1] and autonomous vehicles [2] for a reduction of traffic accidents and an increase of mobile efficiency in terms of energy, time and resources. The history of the autonomous vehicle can be traced back to its first successful implementations in the 1980s by the pioneer institutions in autonomous vehicle, Carnegie Mellon University [3]. In recent years, autonomous vehicles have been a research trend in automotive field. Many notable automotive companies have been conducting researches and technology advances in producing smart autonomous vehicles [2]. For practical implementation, the overall autonomous system should consist of three basic stages and modules which are sensing and perception, planning and path following control.

The study on the motion control of vehicles with dynamic parameter uncertainties has a rich achievement (see, e.g. the recent results in [4–6]) and the employment of advanced control provides vehicles with an ability of driving tasks under vehicle modelling uncertainties. The recent advances in several control schemes occur in autonomous vehicles [7–9] integrate information, sense and control techniques to benefit the minimisation of risks, the improvement of mobility and ease of drivers. The control schemes against dynamic uncertainties, e.g. tyre stiffness and load inertia, are characterised by the use of robust H_∞ control [10–12], sliding model control [13], non-linear control [14], active disturbance rejection control [15] and model predictive control [16, 17]. The prominent part of these control schemes should be the path following control with adaptivity or robustness against model uncertainties.

At the present stage, one may say that the control issues of autonomous vehicles under model uncertainties are fully addressed, as can be seen in the above-mentioned results; however, it remains unclear about the performance of the non-linear vehicle dynamics in the sense that some control issues regarding the tracking accuracy and transient response are not adequately studied. In addition, the issues concerning the application to path following with a non-linear coordinated longitudinal and lateral controller are seldom addressed, especially in the presence of kinematic uncertainty. In fact, the performance of the rapidly developing vision system for automotive applications, as stated in [18–20], is not desirable when key parameters in the camera's calibration drift with the change of vehicle's movements (such as road gradient, suspension height, lateral oscillation). The uncertain measurement on the vehicle longitudinal velocity was considered by [21, 22] and then a gain-scheduling state estimation and/or fault detection scheme was proposed based on the uncertain parameter-varying model. One commonly adopted control approach is the robust H_∞ control [10] for the problem of path following, which can regulate the controlled outputs robust against the uncertainties of the tyre cornering stiffness and the road curvature. However, it seems much more conservative than non-linear control, and the gain selection is for the worst case.

It is well known that the performance of a strict-feedback non-linear system is ensured by appropriately constructing the controller of integrator back-stepping. For automotive vehicle systems, this is almost not achievable except for the known parameter case. In [14], a non-linear coordinated steering and braking controller was applied for the emergency obstacle avoidance of vision-based autonomous vehicles. Nevertheless, the issue about model uncertainties is absent, and the design procedure of the back-stepping controller may seem too complicated for calibration engineers. From the viewpoint of application, the triple-step non-linear control technique was recently developed in automobile control systems [23–25]. The procedure from the control-oriented model to the final implementation of a triple-step controller mainly consists of three design steps: (a) steady-state control, (b) reference variation-based feed-forward control, and (c) tracking error feedback control. This standard idea helps application engineers to select and calibrate a non-linear proportion integration differentiation (PID) controller with the state-dependent parameters. However, it is unclear how to ensure the performance of the vehicle system under both the kinematic and dynamic uncertainties. There is also some work addressing the disturbance rejection problem in the triple-step control (TSC) framework [26] for motors, yet the method cannot expand to the path following problem of autonomous vehicles.

In this study, we propose a modified TSC approach to resolve the path following problem of autonomous vehicles with both uncertain kinematics and dynamics, and the proposed approach addresses both the issue of the system performance and that of engineering applications. A novel controller design scheme is proposed, and it is shown to have the modularisation property, in which the reference generator, adaptive update laws and triple-step

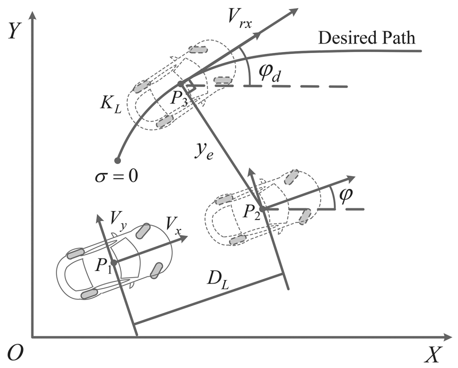

Fig. 1 *Schematic diagram of path following model*

controller are designed independently. The superior/desirable properties of the proposed approach are summarised as follows:

- The design procedure is engineering-oriented, which helps engineers to calibrate a non-linear PID controller with the state-dependent parameters. In practice, this possibility of introducing the modular design methodology of a control loop in the early project phase is very important and valuable for application.
- The proposed controller with appropriate adaptive update laws strengthens the closed-loop system, by which the existing TSC scheme [23] is capable of handling both mulitple input multiple output (MIMO) and model uncertainties, without the expense of conservative gain selection.
- It realises the separation design of the kinematic and dynamic loops such that the adaptive law has explicit physical features with plug-and-play ability. The number of parameter estimates is equal to the number of unknown parameters.

The paper is organised as follows. The modelling of path following and vehicle dynamics is presented in Section 2. Section 3 presents the proposed control scheme. The stability, robustness and tracking performance of the controller are verified. Then in Section 4, the results of the simulation tests performed to validate the path following control performance are presented.

2 Autonomous vehicle modelling

2.1 Vehicle kinematics

Three coordinate systems are usually used to model the path following kinematics of ground vehicles, i.e. the inertial fixed reference coordinate, the path coordinate reference frame, and the body-fixed reference frame.

The vehicle kinematics are shown Fig. 1, where y_e denotes the lateral offset from the preview vehicle centre of gravity P_2 to the straightforward point P_3 on the desired path, and the symbol φ_e is defined as the angular error between the actual heading angle φ and the desired heading angle φ_d. Note that $\varphi_e = \varphi_d - \varphi$ and $\dot{\varphi} = \Omega_z$ with Ω_z being the yaw rate of vehicle. Furthermore, the longitudinal and lateral velocities of vehicle are denoted as V_x and V_y of point P_1, respectively. $\sigma > 0$ denotes the path coordinate (arc-length) of point P_3 along the path from an initial position and K_L represents the curvature of the desired path at the point P_3.

By means of Serret–Frenet equation [27], the path following kinematics of vehicle can be modelled as follows:

$$\begin{cases} \dot{\varphi}_e = V_x K_L - \Omega_z, \\ \dot{y}_e = V_x \sin\varphi_e - V_y \cos\varphi_e - D_L \Omega_z, \end{cases} \tag{1}$$

where D_L denotes a look-ahead distance. Note that the measurement values of the lateral offset y_e and the angular error φ_e can be similar obtained from the vision-based servo system [28]. To facilitate the controller design, the above equation can be rewritten as

$$\begin{cases} \dot{\varphi}_e = K_L V_x - \Omega_z, \\ \dot{y}_e = V_x \varphi_e - V_y - D_L, \Omega_z + d_1 \end{cases} \tag{2}$$

where $d_1 = V_x(\sin\varphi_e - \varphi_e) + V_y(1 - \cos\varphi_e)$.

2.2 Vehicle dynamics

A vehicle model is described as follows. By discounting vertical, roll, and pitch motion, approximating the lateral tyre force as a linear model with respect to the sideslip angle, and ignoring the effect of suspension on the tyre axles, the model used for controller design with three degrees of freedom can be described in terms of dynamics on longitudinal velocity, lateral velocity and yaw rate, e.g.

$$\begin{cases} \dot{V}_x = V_y \Omega_z + \theta_1 V_x^2 + \theta_6 u_1 + d_2, \\ \dot{V}_y = \theta_2 \dfrac{V_y}{V_x} - V_x \Omega_z + \theta_3 \dfrac{\Omega_z}{V_x} + \theta_7 u_2 + d_3, \\ \dot{\Omega}_z = \theta_4 \dfrac{V_y}{V_x} + \theta_5 \dfrac{\Omega_z}{V_x} + \theta_8 u_2 + d_4, \end{cases} \tag{3}$$

where $u = [u_1, u_2]^T$ describes the driving and/or braking torque $u_1 = T_d$ and the controlled front wheel steering angle $u_2 = \delta_f$, respectively. The lumped parameters in (3) are described as $\theta_1 = -C_a/M$, $\theta_2 = -(C_f + C_r)/M$, $\theta_3 = (C_r l_r | - C_f l_f)/M$, $\theta_4 = (C_r l_r - C_f l_f)/I_z$, $\theta_5 = -(C_f l_f^2 + C_r l_r^2)/I_z$, $\theta_6 = 1/MR_e$, $\theta_7 = C_f/M$ and $\theta_8 = C_f l_f/I_z$, where M is the mass of the vehicle, I_z is the vehicle yaw inertia, C_a is the aerodynamic drag term. l_f and l_r are the distances of the front and rear axles from the centre of gravity (CG), respectively. C_f and C_r are the cornering stiffness of the front and rear tyres, respectively. d_2, d_3 and d_4 denote the external disturbances caused by un-modelled dynamics.

2.3 Model uncertainties

One source of dynamics uncertainties results from the change of road conditions and vehicle states. The vehicle mass M may change due to the payload change. According to [29], the moment of inertia is proportional to the mass, thus the uncertain moment of inertia should be considered.

Another kind of significant dynamics uncertainty derives from vehicle tyres. Normally, the tyre-cornering stiffness is treated as a known constant parameter to facilitate the controller design. Nevertheless, it should be important to note that the tyre-cornering stiffness can be affected by many factors such as the normal vertical force, slip angle [6, 10]. For a trade-off between modelling complexity and control flexibility, we are going to give the nominal value of the tyre-cornering stiffness and deal with its uncertainty by adaptive techniques.

Different from dynamics, the uncertainties in the vehicle kinematics mainly come from the visual servo system. As discussed in [18, 28], even though the camera parameters are obtained precisely, the real preview distance D_L may drift with the change of extrinsic parameters. Taking an example illustrated in Fig. 2, assume that the body-fixed reference frame and the camera-fixed reference frame share the common origin and Y-axis, but have different X-axis and Z-axis. Note that the nominal preview distance D_{L0} is measured by the central line of the field of view (the dotted line), i.e. $D_{L0} = h\cot\alpha$ where α and h are the camera-fixed angular and height, respectively. However, due to the overlap of the uneven road, the measured preview distance turns to D_L. In general, there exist more knowledge on the dynamic calibration of on-board camera parameters [18, 28]. From the control viewpoint, a kinematics uncertainty in D_L can be used to describe this problem alternatively.

3 TSC scheme

In this section, we investigate the triple-step controller design for path following of autonomous vehicles given by (2) and (3). The control objective is to ensure the robustly asymptotic convergence

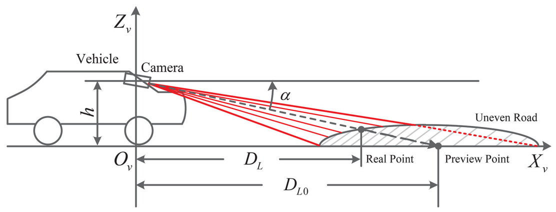

Fig. 2 *Schematic of visual servo system*

of the longitudinal and lateral tracking errors, i.e. $V_x - V_{rx} \to 0$ and $y_e \to 0$ as the desired K_L trajectory, $d \in \mathscr{H}_2 \cap \mathscr{H}_\infty$ and $t \to \infty$, where V_{rx} denotes the desired longitudinal velocity trajectory.

3.1 Reference generator

The main idea of the triple-step method can be demonstrated by considering a class of single input single output systems in control input and control output. However, the input–output formulation may be unacceptable for a kind of MIMO case with different orders, especially for the path following control, in which one faces both the second-order lateral equation and the first-order longitudinal equation. To solve this problem, we are going to design a synthetic reference V_{rs} for MIMO triple-step non-linear controller design.

Notice that the lateral goal of path following is to set y_e to be zero. So the first error e_1 is defined from the lateral error as $e_1 = y_e$. Considering the kinematics uncertainty, we choose the integral Lyapunov function as

$$V_1 = \frac{1}{2}\left(e_1^2 + k_{01}\chi_1^2\right) + \frac{1}{2\kappa_0}\tilde{D}_L^2 \tag{4}$$

with $\chi_1 = \int e_1 \mathrm{d}t$, $k_{01} > 0$ and $\tilde{D}_L = D_L - \hat{D}_L$, and the time derivative of V_1 can be easily calculated as

$$\begin{aligned}\dot{V}_1 = {} & e_1\left[V_x\varphi_e - V_y - \hat{D}_L\Omega_z + d_1 + k_{01}\chi_1\right] \\ & -\frac{1}{\kappa_0}\tilde{D}_L\left(\kappa_0 e_1\Omega_z - \dot{\hat{D}}_L\right)\end{aligned} \tag{5}$$

To eliminate $\tilde{D}_L$ from $\dot{V}_1$, the update law is selected as

$$\dot{\hat{D}}_L = \kappa_0 \mathrm{Proj}_{D_L}(e_1\Omega_z), \tag{6}$$

where $\mathrm{Proj}_a(b)$ is the parameter projection to the variable a such that $\{b = b_{\max}, b > 0\}$ or $\{b = b_{\min}, b < 0\} \to \mathrm{Proj}_a(b) = 0$, or $\mathrm{Proj}_a(b) = b$ otherwise.

In (5), we denote the term $V_s = V_x\varphi_e - \hat{D}_L\Omega_z$ as the virtual control variable, whose dynamics can be calculated as

$$\begin{aligned}\dot{V}_s &= \dot{V}_x\varphi_e + V_x\dot{\varphi}_e - \hat{D}_L\dot{\Omega}_z - \dot{\hat{D}}_L\Omega_z \\ &= \left(V_y\Omega_z + \theta_1 V_x^2 + \theta_6 u_1 + d_2\right)\varphi_e + V_x\dot{\varphi}_e \\ &\quad -\hat{D}_L\left(\theta_4\frac{V_y}{V_x} + \theta_5\frac{\Omega_z}{V_x} + \theta_8 u_2 + d_4\right) - \kappa_0 e_1\Omega_z^2 \\ &= \mathscr{F}_2 + \mathscr{G}_2 u_1 + \mathscr{G}_3 u_2 + d_5,\end{aligned} \tag{7}$$

where

$$d_5 = \varphi_e d_2 - \hat{D}_L d_4, \mathscr{G}_2 = \theta_6\varphi_e, \mathscr{G}_3 = -\theta_8\hat{D}_L$$
$$\mathscr{F}_2 = (V_y\Omega_z + \theta_1 V_x^2)\varphi_e + V_x\dot{\varphi}_e - \hat{D}_L(\theta_4 V_y/V_x + \theta_5\Omega_z/V_x) - \kappa_0 e_1\Omega_z^2$$

Note that the condition for which e_1 tends to zero is that $\dot{V}_1 = -k_1 e_1^2 < 0$ with $k_1 > 0$. Thus, the desired reference V_{rs} can be determined by

$$V_{rs} = -k_1 e_1 - k_{01}\chi_1 + V_y \tag{8}$$

Denote $e_3 = V_{rs} - V_s$ and the error dynamics of e_1 is governed by

$$\begin{aligned}\dot{e}_1 &= V_s - V_y - \tilde{D}_L\Omega_z + d_1 \\ &= -k_1 e_1 - k_{01}\chi_1 - e_3 - \tilde{D}_L\Omega_z + d_1\end{aligned} \tag{9}$$

It should be emphasised that V_{rs} in (8) and V_{rx} formulate the output vector of the reference generator module to the following control module.

3.2 Triple-step controller

The TSC law mainly consists of the following three design procedures.

Step 1: steady-state control. Inspired by the look-up table-based control law that is widely used in automotive engineering, the alternative steady-state control is developed as u_s while retaining the basic function of the conventional look-up tables. For a steady-state control without disturbance, all the transient dynamics take $\dot{V}_x = 0$ and $\dot{V}_s = 0$, respectively, which leads to

$$0 = \mathscr{F}_1 + \mathscr{G}_1 u_1 \tag{10a}$$

$$0 = \mathscr{F}_2 + \mathscr{G}_2 u_1 + \mathscr{G}_3 u_2 \tag{10b}$$

with $\mathscr{F}_1 = V_y\Omega_z + \theta_1 V_x^2$ and $\mathscr{G}_1 = \theta_6$. Since θ are replaced by the estimates $\hat{\theta}$, the steady output-feedback control is obtained as

$$u_s = \begin{bmatrix} u_{s1} \\ u_{s2} \end{bmatrix} = -\begin{bmatrix} \hat{\mathscr{G}}_1 & 0 \\ \hat{\mathscr{G}}_2 & \hat{\mathscr{G}}_3 \end{bmatrix}^{-1}\begin{bmatrix} \hat{\mathscr{F}}_1 \\ \hat{\mathscr{F}}_2 \end{bmatrix} \tag{11}$$

where $\hat{\mathscr{F}}_1 = \mathscr{F}_{1|\theta = \hat{\theta}}$, $\hat{\mathscr{F}}_2 = \mathscr{F}_{2|\theta = \hat{\theta}}$, $\hat{\mathscr{G}}_1 = \hat{\theta}_6$, $\hat{\mathscr{G}}_2 = \hat{\theta}_6\varphi_e$ and $\hat{\mathscr{G}}_3 = -\hat{\theta}_8\hat{D}_L$.

Step 2: reference variation-based feed-forward control. Retaining the steady-state control, we augment the control as $u = u_s + u_f$. Since it is necessary for a fast transient response, by enforcing $\dot{V}_x = \dot{V}_{rx}$ and $\dot{V}_s = \dot{V}_{rs}$, the control u_f is thus derived as

$$u_f = \begin{bmatrix} u_{f1} \\ u_{f2} \end{bmatrix} = \begin{bmatrix} \hat{\mathscr{G}}_1 & 0 \\ \hat{\mathscr{G}}_2 & \hat{\mathscr{G}}_3 \end{bmatrix}^{-1}\begin{bmatrix} \dot{V}_{rx} \\ \dot{V}_{rs} \end{bmatrix} \tag{12}$$

Step 3: tracking error feedback control. Following steps 1 and 2, it is direct to impose the path following by completing the control law

$$u = u_s + u_f + u_e \tag{13}$$

with a feedback control law u_e. Define the tracking errors as $e_2 = V_{rx} - V_x$ and $e_3 = V_{rs} - V_s$. To the objective of path following, one can choose a non-linear Proportional–integral feedback control as

$$u_e = \begin{bmatrix} u_{e1} \\ u_{e2} \end{bmatrix} = \begin{bmatrix} \hat{\mathscr{G}}_1 & 0 \\ \hat{\mathscr{G}}_2 & \hat{\mathscr{G}}_3 \end{bmatrix}^{-1}\begin{bmatrix} k_2 e_2 + k_{02}\chi_2 \\ -e_1 + k_3 e_3 \end{bmatrix} \tag{14}$$

with $\chi_2 = \int e_2 \mathrm{d}t$, $k_2, k_3, k_{02} > 0$. Then substituting the control law (11), (12) and (14) in the dynamical model on e_2 and e_3 leads to

$$\begin{bmatrix} \dot{e}_2 \\ \dot{e}_3 \end{bmatrix} = \begin{bmatrix} \mathscr{E}_1 \\ \mathscr{E}_2 \end{bmatrix} + \begin{bmatrix} \tilde{\mathscr{F}}_1 \\ \tilde{\mathscr{F}}_2 \end{bmatrix} + \begin{bmatrix} \tilde{\mathscr{G}}_1 & 0 \\ \tilde{\mathscr{G}}_2 & \tilde{\mathscr{G}}_3 \end{bmatrix}\begin{bmatrix} u_1 \\ u_2 \end{bmatrix} \tag{15}$$

where

$$\mathscr{E}_1 = -k_2 e_2 - k_{02}\chi_2 - d_2$$

$$\mathscr{E}_2 = -k_3 e_3 + e_1 - d_5$$

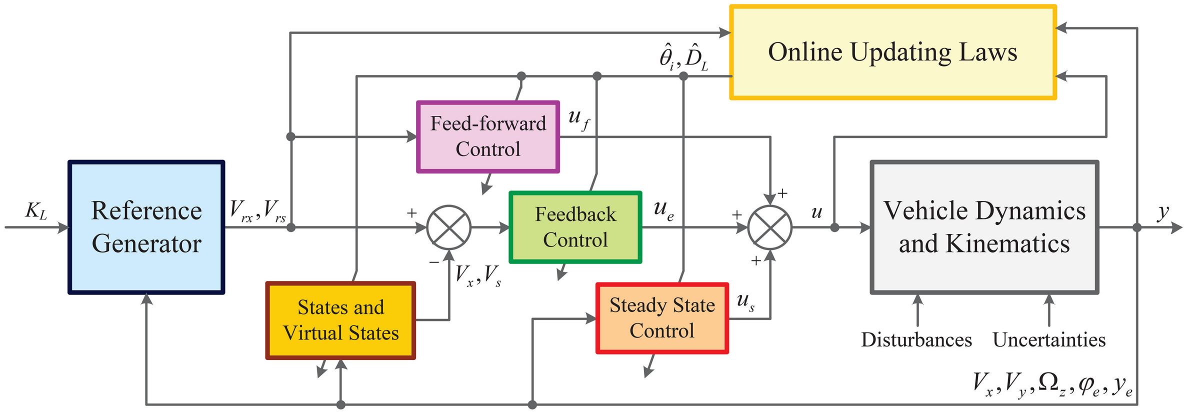

Fig. 3 *Proposed adaptive TSC system for path following of autonomous vehicles*

$$\tilde{\mathscr{F}}_1 = \mathscr{F}_1 - \hat{\mathscr{F}}_1 = \tilde{\theta}_1 V_x^2$$

$$\tilde{\mathscr{F}}_2 = \mathscr{F}_2 - \hat{\mathscr{F}}_2 = \tilde{\theta}_1 V_x^2 \varphi_e - \hat{D}_L \tilde{\theta}_4 (\frac{V_y}{V_x}) - \hat{D}_L \tilde{\theta}_5$$

$$\tilde{\mathscr{G}}_1 = \mathscr{G}_1 - \hat{\mathscr{G}}_1 = \tilde{\theta}_6$$

$$\tilde{\mathscr{G}}_2 = \mathscr{G}_2 - \hat{\mathscr{G}}_2 = \tilde{\theta}_6 \varphi_e$$

$$\tilde{\mathscr{G}}_3 = \mathscr{G}_3 - \hat{\mathscr{G}}_3 = -\tilde{\theta}_8 \hat{D}_L$$

with $\tilde{\theta}_i = \theta - \hat{\theta}$.

To eliminate the above parameter errors, the dynamics update laws are given as follows:

$$\begin{cases} \dot{\hat{\theta}}_1 = -\kappa_1 \mathrm{Proj}_{\theta_1}\left(V_x^2(e_2 + \varphi_e e_3)\right) \\ \dot{\hat{\theta}}_4 = \kappa_4 \mathrm{Proj}_{\theta_4}\left(\hat{D}_L \frac{V_y}{V_x} e_3\right) \\ \dot{\hat{\theta}}_5 = \kappa_5 \mathrm{Proj}_{\theta_5}\left(\hat{D}_L \frac{\Omega_z}{V_x} e_3\right) \\ \dot{\hat{\theta}}_6 = -\kappa_6 \mathrm{Proj}_{\theta_6}(u_1(e_2 + \varphi_e e_3)) \\ \dot{\hat{\theta}}_8 = \kappa_8 \mathrm{Proj}_{\theta_8}\left(\hat{D}_L u_2 e_3\right) \end{cases} \tag{16}$$

3.3 Stability analysis

In the following theorem, the adaptive triple-step non-linear control scheme is developed for the path following purpose when both the kinematics item D_L and the dynamics item θ exhibit uncertainties.

Theorem 1: Consider the system given by (2) and (3). Select the TSC law (13) with the reference generator (8) as well as the kinematics update law of (6) and the dynamics update law of (16). Select k_i satisfying the conditions:

$$k_i = \frac{1}{2}\left(\lambda_i + \frac{1}{\gamma^2}\right), \quad \lambda_i > 0, \quad \gamma > 0, \quad i = 1, 2, 3 \tag{17}$$

Then the closed-loop system satisfies:

(a) For any initial value the following quadratic performance criterion is achieved:

$$\int_0^\infty \| e \|_Q^2 \, \mathrm{d}t \le \| e(0) \|_Q^2 + \| \tilde{\theta}(0) \|_K^2 + \gamma^2 \int_0^\infty \| d \|^2 \, \mathrm{d}t \tag{18}$$

with

$$K = \mathrm{diag}([\kappa_0, \kappa_1, \kappa_4, \kappa_5, \kappa_6, \kappa_8]), \mathscr{J} = \{1, 4, 5, 6, 8\}$$

$$Q = \mathrm{diag}([\lambda_1, \lambda_2, \lambda_3]), \theta^{\mathrm{T}} = [D_L, \theta_1, \theta_4, \theta_5, \theta_6, \theta_8]$$

.

(b) If the disturbance is square-integrable and bounded, i.e. $d \in \mathscr{L}_2[0, \infty) \cap \mathscr{L}_\infty[0, \infty)$, then $\lim_{t \to \infty} e(t) = 0$.

Proof: Choose the Lyapunov function candidate as

$$V = \sum_{i=1}^{3} \frac{1}{2} e_i^2 + \sum_{i=1}^{2} \frac{k_{0i}}{2} \chi_i^2 + \frac{1}{2\kappa_0} \tilde{D}_L^2 + \sum_{j \in \mathscr{J}} \frac{1}{2\kappa_j} \tilde{\theta}_j^2 \tag{19}$$

Taking the time derivative of V along the error dynamics (15), (6) and (16) and cancelling integral and unknown parameter terms, we have

$$\begin{aligned} \dot{V} = {} & e_1\left(-k_1 e_1 - k_{01}\chi_1 - e_3 - \tilde{D}_L \Omega_z + d_1\right) \\ & + e_2\left(-k_2 e_2 - k_{02}\chi_2 - d_2 + \tilde{\mathscr{F}}_1 + \tilde{\mathscr{G}}_1 u_1\right) \\ & + e_3\left(-k_3 e_3 + e_1 - d_5 + \tilde{\mathscr{F}}_2 + \tilde{\mathscr{G}}_2 u_1 + \tilde{\mathscr{G}}_3 u_2\right) \\ & + k_{01} e_1 \chi_1 + k_{02} e_2 \chi_2 + \tilde{D}_L e_1 \Omega_z \\ & - \tilde{\theta}_1 V_x^2 (e_2 + \varphi_e e_3) - \tilde{\theta}_4 \hat{D}_L \frac{V_y}{V_x} e_3 \\ & - \tilde{\theta}_5 \hat{D}_L \frac{\Omega_z}{V_x} e_3 - \tilde{\theta}_6 u_1 (e_2 + \varphi_e e_3) - \tilde{\theta}_8 \hat{D}_L u_2 e_3 \\ = {} & -e_1(k_1 e_1 + e_3 + d_1) - e_2(k_2 e_2 + d_2) \\ & - e_3(k_3 e_3 - e_1 + d_5) \\ = {} & -\frac{1}{2} e^{\mathrm{T}} Q e - \sum_{i=1}^{2} \frac{1}{2}\left(\frac{1}{\gamma} e_i + \gamma d_i\right)^2 \\ & - \frac{1}{2}\left(\frac{1}{\gamma} e_3 + \gamma d_5\right)^2 + \frac{1}{2}\gamma^2\left(d_1^2 + d_2^2 + d_5^2\right) \\ \le {} & -\frac{1}{2} e^{\mathrm{T}} Q e + \frac{1}{2}\gamma^2 d^{\mathrm{T}} d \end{aligned} \tag{20}$$

Integrating the above inequality from $t = 0$ to ∞ leads to (18), and if $d \in \mathscr{L}_2[0, \infty) \cap \mathscr{L}_\infty[0, \infty)$, using the Barbalat's lemma, then the performance of robustly asymptotically tracking holds. Thereby, the proof is completed. □

By combining the reference generator (8) with the control law in (13) and the update laws (6), (16), the adaptive triple-step coordinated control scheme for path following of autonomous vehicles can be realised as shown in Fig. 3.

Remark 1: Except the steady-state control u_s concerning the state-dependent steady compensation, the feedback control u_e embodies the proportional and integral items, while the feed-forward control u_f involves the derivative items $\dot{e}_1$. Hence, the derived TSC law is consistent with the form of PID control in which the control gains are state-dependent. The obtained control law presents a controller structure which is simple and intuitive. It

Table 1 Vehicle parameters used in the simulation

Symbol	Description	Values (units)
M	nominal vehicle mass	1360 kg
I_z	nominal inertia moment of vehicle on yaw rate	1993 $\mathrm{kg\,m^2}$
l_f	distance of CG from front axle	1.45 m
l_r	distance of CG from rear axle	1.06 m
C_a	aerodynamic drag coefficient	0.5 $\mathrm{N\,s^2/m^2}$
R_e	tyre effective rolling radius	0.33 m
C_f	front cornering stiffness	151 kN/rad
C_r	rear cornering stiffness	146 kN/rad
μ	tyre–road friction coefficient	0.8
D_L	nominal look-ahead distance	10 m

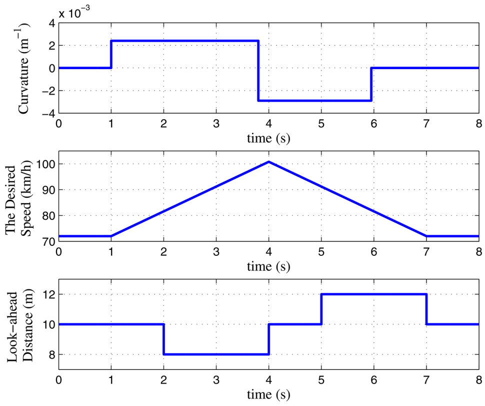

Fig. 4 *Reference path and* D_L

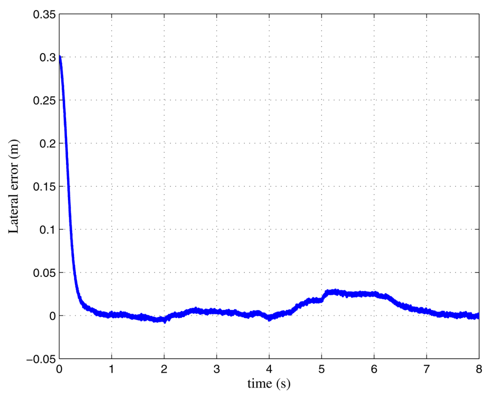

Fig. 5 *Lateral errors*

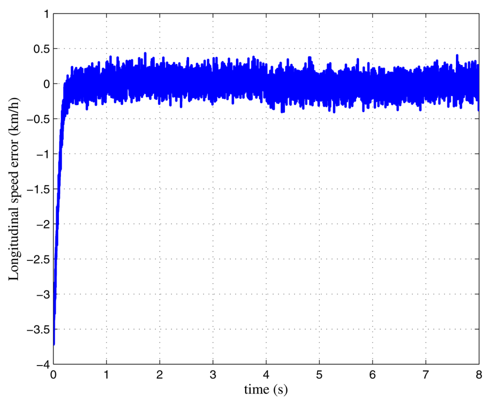

Fig. 6 *Longitudinal speed errors*

is worth mentioning that the proposed control law not only inherits the merits of the conventional triple-step non-linear method [23], but also provides the adaptability and a quantified guideline for tuning feedback parameter k_i, which guarantees the H_∞ tracking offset for arbitrary bounded disturbances.

Remark 2: In the proposed scheme, the TSC for non-linear systems can be generalised to integrator MIMO systems. Thanks to the use of a reference generator, the issue of exploitation of the terms for high-order non-linear systems is avoided in the triple-step design procedure. Besides, the proposed adaptive controller achieves separation by using a feedback of the virtual control variable V_s with the estimate $\hat{D}_L$. Due to this, the adaptive update law for dynamics parameters θ_j is applicable without the real D_L and the number of parameter estimates is minimised to the number of unknown parameters. It should be mentioned that the control law in Theorem 1 can only guarantee the convergence of tracking error, while the parameter convergence may be not available because the persistent excitation does not often hold in the closed-loop operation.

4 Benchmark simulations

The control performance is tested with two-lane change manoeuvers and one J-turn manoeuver via benchmark simulation using a high-fidelity full-vehicle model constructed in VeDYNA® and Matlab/Simulink. Those vehicle longitudinal forces, tyre lateral forces and aligning moments as the functions of the slip angle and longitudinal slip ratio are generated by the UniTire model, where tyre normal loads are calculated from the total mass of tyre, wheel and vehicle acceleration. Representative model parameters are shown in Table 1.

To improve the validation of simulation, both measurement noise and actuator dynamics are considered. First, the measured yaw rate, lateral and longitudinal speeds are assumed to be contaminated with noise ($S/N = 10$). Second, we assume that there is the torque controller for each actuator and the ideal close-loop system is simplified as $T_d = 1/(\tau s + 1)T_c$, where $\tau = 0.01$ is the closed-loop response time, which is a control characteristic of the controller, and T_c is drive torque command. Consequently, the gains for the lane change simulation are selected as $k_1 = 20$, $k_{01} = 50$, $k_2 = 10$, $k_{02} = 10$ and $k_3 = 15$.

4.1 Single-lane change manoeuver

In the single-lane change manoeuver, the vehicle is made to complete a large lane-change manoeuver with a desired longitudinal load on a high adherence road with $\mu = 0.8$. To demonstrate the simultaneous longitudinal and lateral manoeuver with kinematic uncertainty, the look-ahead distance, the reference speed and the real look-ahead distance are presented in Fig. 4. The initial lateral and velocity errors are set to 0.3 m and 3.6km/h, respectively.

Fig. 5 reveals the response result of the lateral error, it can be seen that the maximum steady-state error of the proposed control system is bounded to ± 0.03 m, which occurs in the largest curvature of $-0.0029\ \mathrm{m^{-1}}$ and the largest look-ahead distance of 12 m. Besides, the longitudinal speed error trajectory is shown in Fig. 6, it is clear that the response of the longitudinal velocity basically coincided with the desired values.

The results of the corresponding driving torque and front wheel steering angle are shown in Fig. 7. From these trajectories, one can see that the system inputs are maintained in reasonable regions. The global trajectory of the path following is shown in Fig. 8. It is found that the lane change manoeuver of path following is fulfilled satisfactorily, and thus the good performance of the proposed adaptive triple-step controller in the presence of uncertain kinematics and dynamics can be verified.

4.2 Quantitative analysis in other manoeuvers

In the following simulation cases, the vehicle is made to complete a double-lane change manoeuver and a J-turn manoeuver, respectively. The double-lane change test consists of an entry and an exit lane with a length of 12 m and a side lane with a length of

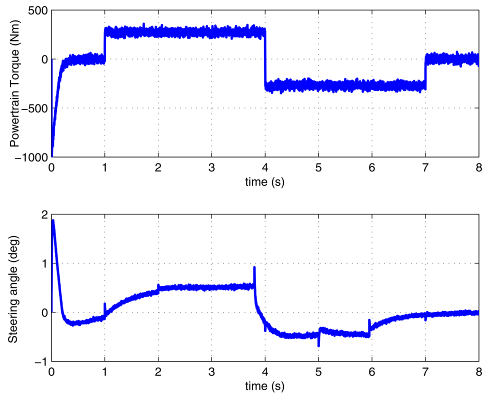

Fig. 7 *Powertrain torque and steering angle trajectories*

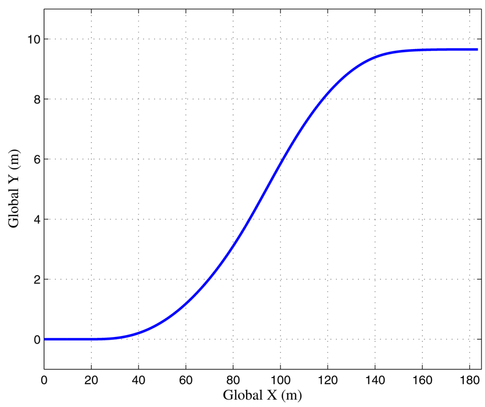

Fig. 8 *Global trajectory*

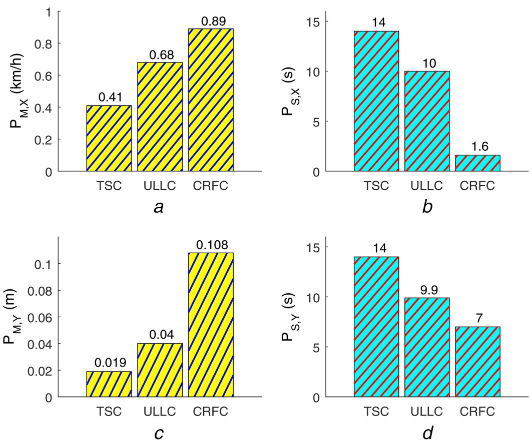

Fig. 9 *Indices P_{M} and P_{S} in the double-lane change manoeuver*

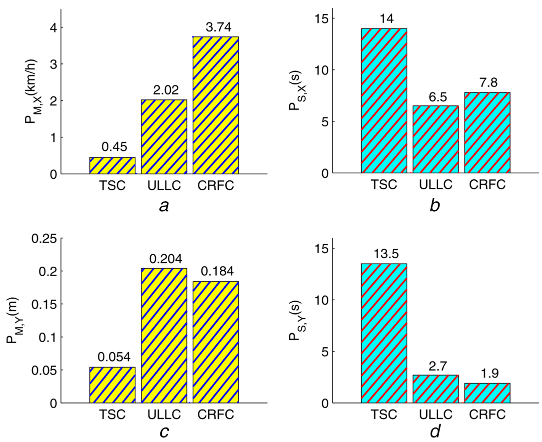

Fig. 10 *Indices P_{M} and P_{S} in the J-turn manoeuver*

11 m. The width of the entry and side lane is dependent on the width of the vehicle, the width of the exit lane is constantly 3 m wide. The velocity reference is increased gradually from 118 up to 125 km/h at 5 s, and then decreased linearly to 114 km/h. The curvature for path following is calculated from the ratio between the experiential yaw rate and the velocity reference. The J-turn manoeuver considers a step curvature input with the amplitude $0.007\,\mathrm{m}^{-1}$ that is made rapidly to maximumly excite the dynamics of the vehicle. The velocity reference is set as a sine signal with bias 72 km/h, amplitude 11 km/h and frequency 0.25π rad/s. The look-ahead distance changes from 10 to 5 m.

To quantitative analysis, the results are further compared with the uncoordinated longitudinal and lateral control (ULLC) [9] and the coordinated robust feedback control (CRFC) [10]. In assessing the performance of these three schemes, two important criteria should be considered, i.e. the maximum error absolute (P_{M}) and the satisfactorily accomplished missions (P_{S})

$$P_{\mathrm{M},i} = \sup_{t \in [0, T_{\mathrm{total}}]} |e_i(t)|, \quad P_{\mathrm{S},i} = T_{\mathrm{sat},i} \; i = X, Y$$

with respect to the double-lane change and J-turn manoeuvers.

These two indices quantitatively state how efficient the controller is. According to simulation tests, the total time period T_{total} is 14 s. T_{sat} denotes the sum of the time period during which the lateral tracking accuracy is within 0.02 m, and its longitudinal tracking error is within 0.5 km/h. T_{sat} is very crucial and is to be maximised so that the performance of tracking accuracy and transient response can be evaluated. The larger T_{sat} is, the better dynamics performance can be indicated. In addition, the larger $P_{\mathrm{M},i}$ is, the worse performance caused by uncertainties and abrupt distances is able to be evaluated during the path following control.

In the absence of initial state errors, the corresponding performance of index P_{M} and that of P_{S} are shown in Figs. 9 and 10. The following remarks are found.

(1) Although ULLC in the double-lane change can achieve similar values P_{M} (as shown in Figs. 9*a* and *c*) as TSC by tuning the gains of ULLC. The index value P_{S} that was obtained from the ULLC is smaller than that from TSC. As depicted in Fig. 10, both performance indices of TSC are apparently better than those of ULLC in the J-turn manoeuver. This is because, although ULLC is able to handle vehicle non-linear dynamics and external disturbances, it is actually an uncoordinated control scheme, in which the coupled effects between the longitudinal and lateral dynamics are neglected. Hence, the performance of ULLC would be degraded. On the other hand, due to the integration of the triple-step non-linear coordinated control scheme and the adaptive update laws for both the uncertain kinematics and dynamics, TSC can have a better stability, robustness and disturbance attenuation. As shown in Figs. 9 and 10, the index values P_{S} are more or less the entire time period of manoeuvers.

(2) Since CRFC is only able to solve the path following problem of the autonomous vehicle subject to polyhedral hypothesis, the longitudinal speed, the yaw rate and the path curvature should be limited in the range. As a result, if there occurs some abnormal conditions, e.g. emergency obstacle avoidance, such that the hypothesis is invalid, CRFC may result in no feasible solution, unexpected performance and even instability. Additionally, as shown in Figs. 9 and 10, all values of indices P_{M} and P_{S} are much weaker than those of TSC. Two reasons are explained as follows. First, CRFC is a robust control scheme, hence, its controller has certain conservativeness and only the worst case is considered. Second, the information of feed-forward (reference generator) is not made use of so that the performance of dynamic path tracking is much weaker than that of the proposed TSC and ULLC. That can be verified by the results in Figs. 9 and 10.

(3) In the presence of kinematics uncertainty, TSC has better performance than both ULLC and CRFC. One of important reasons is that TSC is able to handle the changed look-ahead distance, whose essence is to control vehicles with unknown visual servo parameters. One of the improvements to be achieved with TSC

design in this study is the reduction of the dynamic order of the adaptive update law to its minimum. The minimum-order design is advantageous not only for implementation, but also because it guarantees the strongest achievable stability and convergence properties.
(4) Due to the robustness for the uncertainties of actuator gains, TSC can be easily extended to the issue of passive fault-tolerant control that provides emergency steering and driving control against those mild faults of in-wheel motors and/or active steering system.

Based on the above comparisons and analysis, it is seen that the proposed control approach provides better performance than the controllers presented in [9, 10]. It also means that our proposed control scheme can be appealing to realise the path following control of autonomous vehicles with uncertain kinematics and dynamics.

5 Conclusion

We have considered the control problem of path following for autonomous vehicles subject to both the kinematic and dynamic uncertainties. We have proposed a novel control scheme that integrates a reference generator, a triple-step controller and on-line updating laws. The performance is then shown to be conveniently ensured in the sense of modularisation design, with essentially the adaptive MIMO modification of the control law as in [23]. The proposed control scheme introduces the concept of TSC with a minimum number of parameter estimates can be considered as a qualified (or perhaps superior) alternative to the existing path following results.

6 References

[1] Bengler, K., Dietmayer, K., Faerber, B., et al.: 'Three decades of driver assistance systems: review and future perspectives', *IEEE Intell. Transp. Syst. Mag.*, 2014, **6**, (4), pp. 6–22

[2] Amer, N.H., Zamzuri, H., Hudha, K., et al.: 'Modeling and control strategies in path tracking control for autonomous ground vehicles: a review of state of the art and challenges', *J. Intell. Robot Syst.*, 2017, **86**, (2), pp. 225–254

[3] Wallace, R., Stentz, A., Thorpe, C.E., et al.: 'First results in robot road-following'. Proc. IJCAI, CA, USA, 1985, pp. 18–23

[4] Do, M.T., Man, Z., Zhang, C., et al.: 'Robust sliding mode-based learning control for steer-by-wire systems in modern vehicles', *IEEE Trans. Veh. Technol.*, 2014, **63**, (2), pp. 580–590

[5] Jia, Y.M.: 'Robust control with decoupling performance for steering and traction of 4WS vehicles under velocity-varying motion', *IEEE Trans. Control Syst. Technol.*, 2000, **8**, (3), pp. 554–569

[6] Wang, R., Zhang, H., Wang, J.: 'Linear parameter-varying controller design for four-wheel independent actuated electric ground vehicles with active steering systems', *IEEE Trans. Control Syst. Technol.*, 2014, **22**, (4), pp. 1281–1296

[7] Li, X., Sun, Z., Cao, D., et al.: 'Development of a new integrated local trajectory planning and tracking control framework for autonomous ground vehicles', *Mech. Syst. Signal Process.*, 2017, **87**, (SI), pp. 118–137

[8] Wit, J.: 'Autonomous ground vehicle path tracking', *J. Robot. Syst.*, 2004, **21**, (8), pp. 439–449

[9] Xu, L., Wang, Y., Sun, H., et al.: 'Integrated longitudinal and lateral control for Kuafu-II autonomous vehicle', *IEEE Trans. Intell. Transp. Syst.*, 2016, **17**, (7), pp. 2032–2041

[10] Hu, C., Jing, H., Wang, R., et al.: 'Robust H_∞ output-feedback control for path following of autonomous ground vehicles', *Mech. Syst. Signal Process.*, 2016, **70–71**, pp. 414–427

[11] Wang, R., Hu, C., Yan, F., et al.: 'Composite nonlinear feedback control for path following of four-wheel independently actuated autonomous ground vehicles', *IEEE Trans. Intell. Transp. Syst.*, 2016, **17**, (7), pp. 2063–2074

[12] Wang, R., Jing, H., Hu, C., et al.: 'Robust H_∞ path following control for autonomous ground vehicles with delay and data dropout', *IEEE Trans. Intell. Transp. Syst.*, 2016, **17**, (7), pp. 2042–2050

[13] Li, B., Du, H., Li, W.: 'Trajectory control for autonomous electric vehicles with in-wheel motors based on a dynamics model approach', *IET Intell. Transp. Syst.*, 2016, **10**, (5), pp. 318–330

[14] Guo, J., Hu, P., Wang, R.: 'Nonlinear coordinated steering and braking control of vision-based autonomous vehicles in emergency obstacle avoidance', *IEEE Trans. Intell. Transp. Syst.*, 2016, **17**, (11), pp. 3220–3240

[15] Xia, Y., Pu, F., Li, S., et al.: 'Lateral path tracking control of autonomous land vehicle based on adrc and differential flatness', *IEEE Trans. Ind. Electron.*, 2016, **63**, (5), pp. 3091–3099

[16] Fitri, Y., Yasuchika, M.: 'Comparative study of autonomous path-following vehicle control via model predictive control and linear quadratic control', *Proc. Inst. Mech. Eng. D, J. Automob. Eng.*, 2015, **229**, (12), pp. 1695–1714

[17] Gao, Y., Gray, A., Tseng, H.E.: 'A tube-based robust nonlinear predictive control approach to semi-autonomous ground vehicles', *Veh. Syst. Dyn.*, 2014, **52**, (6), pp. 802–823

[18] Bertozzi, M., Broggi, A., Fascioli, A.: 'Vision-based intelligent vehicles: State of the art and perspectives', *Robot. Auton. Syst.*, 2000, **32**, (1), pp. 1–16

[19] Brown, A.A., Brennan, S.N.: 'Lateral vehicle state and environment estimation using temporally reviewed mapped lane features', *IEEE Trans. Intell. Transp. Syst.*, 2015, **16**, (3), pp. 1601–1608

[20] Ponsa, D., Serrat, J., Lopez, A.M.: 'On-board image-based vehicle detection and tracking', *Trans. Inst. Meas. Control*, 2011, **33**, (7), pp. 783–805

[21] Zhang, H., Zhang, G., Wang, J.: 'H_∞ observer design for LPV systems with uncertain measurements on scheduling variables: application to an electric ground vehicles', *IEEE-ASME Trans. Mech.*, 2016, **21**, (3), pp. 1659–1670

[22] Zhang, H., Wang, J.: 'Active steering actuator fault detection for an automatically-steered electric ground vehicle', *IEEE Trans. Veh. Technol.*, 2017, **66**, (5), pp. 3685–3702

[23] Chen, H., Gong, X., Liu, Q., et al.: 'Triple-step method to design nonlinear controller for rail pressure gasoline direct injection engines', *IET Control Theory Appl.*, 2014, **8**, (11), pp. 948–959

[24] Gao, B., Chen, H., Liu, Q., et al.: 'Position control of electric clutch actuator using a triple-step nonlinear method', *IEEE Trans. Ind. Electron.*, 2014, **61**, (12), pp. 6995–7003

[25] Wang, F., Chen, H., Cao, D.: 'Nonlinear coordinated motion control of road vehicles after a tire blowout', *IEEE Trans. Control Syst. Technol.*, 2016, **24**, (3), pp. 956–970

[26] Chu, H., Gao, B., Gu, W.: 'Low-speed control for permanent-magnet dc torque motor using observer-based nonlinear triple-step controller', *IEEE Trans. Ind. Electron.*, 2017, **64**, (4), pp. 3286–3296

[27] Iyer, B.R., Vishveshwara, C.V.: 'Frenet-serret description of gyroscopic precession', *Phys. Rev. D, Part. Fields*, 1994, **48**, (12), pp. 5706–5720

[28] Bertozzi, M., Broggi, A.: 'Gold: A parallel real-time stereo vision system for generic obstacle and lane detection', *IEEE Trans. Image Process.*, 1998, **7**, (1), pp. 62–81

[29] Mammar, S.: 'Two-degree-of-freedom H_∞ optimization and scheduling for robust vehicle lateral control', *Veh. Syst. Dyn.*, 2000, **34**, (6), pp. 401–422